International Journal of Internal Medicine 2012, 1(2): 6-10
DOI: 10.5923/j.ijim.20120102.01

Complications Due to Extracorporeal Shock Wave Lithotripsy and Role of Cavitation Bubbles Impacts

Massoud Malaki[1,*], Amir Abdullah[1], Ebrahim Baghizadeh[1],Zahra Heidari-Chamshiri[2]

[1]Department of Mechanical Engineering, Amirkabir University of Technology, Hafez Ave., Tehran, Iran
[2]Department of Medicine, Jahrom University of Medical Sciences, Fars, Iran

Abstract This paper presents a study of the role played by cavitations' bubbles in the creation of side effects or complications of cavitation bubbles' impact generated by Extracorporeal Shock Wave Lithotripsy (ESWL). Apart from many useful applications of shock waves therapy, specifically, key role of cavitations' bubbles in the disintegration of urinary calculi, there is a large number of complications due to improper cavitations' bubbles intensity applied on the surfaces or organs. For the best result of ESWL with the lowest complications, shock wave intensity should be selected and controlled accurately. The main purpose of this study was to determine the impulse of a bubble on a surface. To do this, the results of previous numerical studies were used to derive a relationship between the speed of microjet and acoustic pressure amplitude. It was found that the speed of microjet is proportional to the logarithm of the acoustic pressure amplitude. Aluminum foil specimens were exposed to cavitation for 3 seconds and the dimensions of permanent pits generated on specimens were measured. Then, the deformation energy of each pit and the corresponding impulse were calculated. The trend of experimental results was in a good agreement with the theoretical ones.

Keywords Complications, ESWL, Cavitation Bubbles' Impact, Kidney

1. Introduction

Extracorporeal shock wave lithotripsy (ESWL) is the use of high-energy shock waves to fragment and disintegrate kidney stones. The shock wave, created by using a high-voltage spark or an electromagnetic impulse, is focused on the stone. This shock wave shatters the stone and this allows the fragments to pass through the urinary system. Since the shock wave is generated outside the body, the procedure is termed extracorporeal shock wave lithotripsy, or ESWL [1].

Lithotripsy uses the technique of focused shock waves in cavitation bubbles' impact to fragment a stone in the kidney or the ureter. The patient is placed in a tub of water or in contact with a water-filled cushion, and a shock wave is created which is focused on the stone. The cavitation bubbles and their impacts shatter and fragment the stone [2]. The resulting debris, called gravel, then passes through the remainder of the ureter, through the bladder, and through the urethra during urination.

In any case, these impacts and activation bubbles have many complications in kidney or in any organ that these side effects are as follow[3].

* Corresponding author:
massoudmalaki@gmail.com (MassoudMalaki)
Published online at http://journal.sapub.org/ijim

2. Complications

However, with the subsequent rapid proliferation of this technology to more and more centers worldwide and the development of second generation lithotripters with smaller focus, lower focal energy and better imaging the interest in the possible complications.

The complications due to cavitation bubbles can be subdivided in traumatic effects and functional effects (Table 1).

Table 1. Complications

Traumatic effects							Functional effects	
Direct exposure to SW				Clinical side effects				
Kidney	Lung	Intestine	Blood Vessels	Gross Hematuria	Skin Bruising	Pain	Kidney	Cardiovascular System

The traumatic effects are due to the direct exposure of organs and tissues to shockwaves. We will consider traumatic effects to kidney, lung, intestine and blood vessels and clinical side effects.

2.1. Traumatic effects to the kidney

The direct impact of micro jets to the kidney causes an effect comparable to a blunt trauma of this organ. In nearly every patient the shockwaves cause a parenchymal edema

[4]. This edema is transitory and dosage dependent. The incidence of parenchymal edema significantly increases when more than 1500 shockwaves are administered [4]. There is less edema when a machine with a small focus is used. The edema spontaneously resolves by 1 week post-ESWL, and therefore subsequent ESWL sessions should be interspaced by approximately 1 week. A subcapsular or perirenal hematoma [4, 5] is a more serious complication of ESWL.

When patients are screened by CT or MRI a subcapsular or perirenal hematoma is diagnosed in 25 - 30 % of cases. However when screened by ultrasound only 0.24 - 0.66 % of patients prove to have a hematoma. These hematomas are considered to be the clinically significant hematomas. A number of factors predispose patients to develop a hematoma: these predisposing factors are outlined in table 2. The most important clinical sign of a hematoma is PAIN. Any abnormal pain post-ESWL should raise the suspicion of the existence of hematoma and should trigger thorough investigation.

Table 2. Prevention of subcapsular and perirenal hematoma

Patient related factors	Check and control blood pressure pre-ESWL
	Check and control blood coagulation pre-ESWL
	Be aware of increased risk in conditions related to generalized atherosclerosis
Lithotripter related factors	Small focus is an advantage
	Real time US imaging guarantees better control of shock wave delivery to stone
Operator related factors	Careful initial targeting and proper surveillance of treatment
	Careful control of total energy given in risk patients:
	Avoid "casual" overtreatment

Careful ultrasonic examination of the flank region will quickly reveal the possible existence of a hematoma, while a CT-scan will give more detailed information on its extent. Both ultrasound and CT-scan will be important in the follow-up of an eventual hematoma. In large hematomas bulging or tendeness of the flank region may be observed. Tachycardia and signs of acute anemia are rare and only seen in very extensive and rapid developing hematomas. Impairment of renal function may be seen in solitary kidneys. As a hematoma is a major complication with possibly severe consequences, the prevention of hematomas is of paramount importance. The prevention basically consists in the control of the predisposing factors as given in table 2. When taking the patients history, it proves to be particularly important to specifically ask for the eventual use of aspirin, as this drug influences blood coagulation, but by most patients is not considered to be a real drug [5]. The treatment even of a large hematoma basically is conservative. Initially a blood transfusion may be necessary. Spontaneous resorption may take 6 weeks to 6 months [6]. Rarely percutaneous or open drainage will be necessary. In large hematomas with extensive laceration of the kidney a nephrectomy may have to be considered.

2.2. Traumatic effects to the lung

Traumatic effects to the lung [7] are very rare (less than 1 %), the risk group being CHILDREN. Clinical signs are those of lung hemorrhage: hemoptysis or, in more severe cases, hemothorax. Trauma to the lung should and easily can be prevented by Styrofoam shielding of the lung area in children and by carefully targeting the shockwaves. When delivering the shockwaves one should be aware of the blast path: the shockwaves do travel beyond the cross on the screen.

2.3. Traumatic effects to intestines

This complication occurs only in less than 1 % of treatments and is most often caused by intestine exposed to the blast path of the shockwaves. Exposure of stomach and duodenum will cause transient mucosal bleeding, while exposure of the pancreas can cause acute pancreatitis with elevated amylase and lipase levels. Again the prevention is overimportant and consists in the careful targeting of the shockwaves always being aware of the blast path [8].

2.4. Traumatic effects to blood vessels

Traumatic effects to blood vessels are extremely rare. Keeler et al. reported on a femoral artery thrombosis several hours after the treatment of a low urteral stone on an unmodified Dornier HM3 [9] while Vandeursen et al. reported on an iliac vein thrombosis following the treatment of a low ureteral stone on a Siemens Lithostar [10].

Atherosclerosis is the predisposing factor and prevention consists in careful targeting in patients with generalized atherosclerosis. One should beware of a calcified or aneurysmatic aorta or artery in the vicinity of the treatment area avoiding direct impact to these vessels. Again awareness of the blast path is important.

2.5. Clinical side effects

Clinical side effects are also due to the direct impact of shockwaves to the kidney and the skin. Gross hematuria is the consequence of direct injury to the renal parenchyma. Although it occurs regardless of the type of lithotripter used, the incidence is lower in machines with a smaller focus. It is transient lasting between 24-48 hours but clots can cause colic. Skin bruising, petechiae or ecchymosis, is largely dependent of the energy density at skin level. Machines with a large aperture will have a larger surface area of shockwave entry, hence a lower energy density per cm2 of skin area and less skin bruising. Higher energy levels will cause more skin bruising. Two types of pain may be experienced by a patient treated with shockwaves: superficial pain at skin level and visceral pain in the kidney. The energy density at skin level

again is the most important factor in superficial pain. Shock wave focus and pressure level of shockwaves are the determinating factors in the deep visceral pain. A lithotripter with a large aperture and a small focus will cause less pain. Proper shockwave targeting is important with any type of lithotripter.

3. Theoretical Investigations

In this section, we have indirectly measured the amount of energy transmitted to the specimen applied to the specimen in acoustic cavitation field.

In spite of difference of aluminum foil and organs of the body, according to [11] aluminum foil is a good material for the measurement of cavitation bubbles impact. If an aluminum foil is exposed to cavitation for a short period of time, permanent dome shaped effects appear on it (Fig. 1) .The amount of energy required to form such permanent domes can be calculated through some formulas used in sheet metal forming processes. Fig. 2 shows a sheet with the initial thickness, t0, which has been clamped on its periphery rigidly and is being bulged by fluid pressure, P. The membrane stresses are illustrated in Fig. 3.

of a sentence.

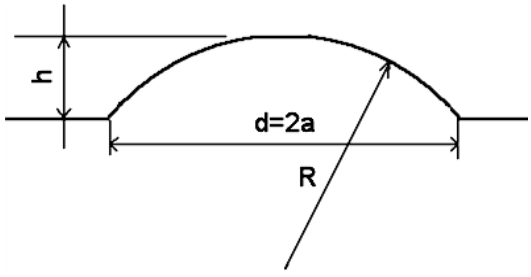

Figure 1. Schematic of a permanent dome shaped effect produced on a specimen as a result of being exposed to cavitation

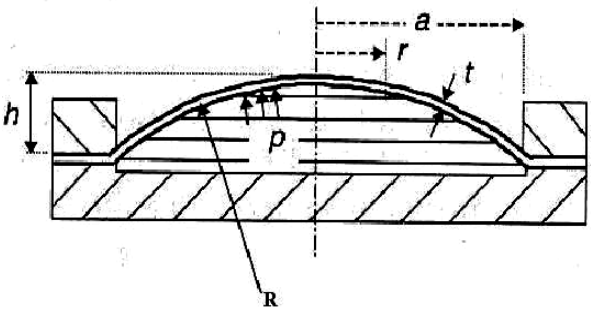

Figure 2. Bulging a thin sheet with fluid pressure

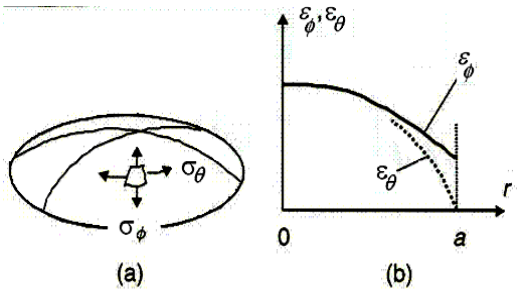

Figure 3.(a) Membrane stresses on the spherical shell, (b) Distribution of membrane strains at some stage in the bulg-ing process

By assuming the symmetry, rigid-perfect plastic behavior for the material and since the volume of formed material does not change before and after deformation and hence the final equation for deformation energy is [12, 13, 14]:

$$W_P = \frac{\pi}{3} Y t_0 a^2 \ln\left[1+\left(\frac{h}{a}\right)^2\right] \quad (1)$$

The impulse can be obtained by the equation 2:

$$I = \sqrt{2\rho\pi a^2 t_0 W_P} \quad (2)$$

Equations 1 and 2 will be used in our experiments to calculate the amount of energy transmitted to specimens and the corresponding impulse applied to the specimens by the bubbles. Where ρ is density of the blank material, t0 is initial thickness, a is the radius of the blank at the periphery where it is clamped, h is the depth of the dome and Y is the yield stress.

4. Experimental investigations

Fig. 4 represents a schematic view of the vibratory cavitation test apparatus for generating the cavitation bubbles. The apparatus consists of an ultrasonic generator (power supply), transducer, horn and specimen holder assembly. The vibrating horn frequency was 23 kHz with a diameter of 4mm. Specimens had dimensions of 70×50mm and were cut from an Aluminum foil, the thickness of which was 15μm and had the yield strength of 34MPa. Specimens were placed at different distances (L) from the horn tip and were tested for duration of 3 seconds. Selected values of L were 2mm, 16mm, 32mm, 48mm and 64mm. Except L=2mm, the rest were equal to ¾ λ and λ; where λ is the acoustic wave length. In the case of L= ½ λ and L=λ, i.e. an integer multiple of ½ λ, a standing wave field was generated between the specimen and the horn tip.

According to [14] the acoustic pressure amplitude which was the result of vibration of the horn tip varies from 15.1atm to 60.4atm and makes the impact load variable.

In practice, no pits appeared on the specimens at L=λ=64mm. At L=48mm only at P=160w some pits appeared on the specimen. So, tests were limited to three cases L=2, 16, 32mm.

4.1. Measurement of the Dimensions of the Pits

As a result of being exposed to cavitation, some dome shaped effects appeared on specimens which hereinafter will be named pits.Dimensions of pits including their depth (h) and their diameter (d) were measured using a LEITZ microscope with magnifications 50 and 100.Fig. 5 shows measuring the depth of the pit schematically. In order to measure its depth, at first, microscope was made to focus on point (1), then its table was displaced to focus on point (2). Displacement of microscope table between these two positions is equal to the depth of the pit. Displacement was measured using a dial indicator with 0.001mm resolution. Suitable magnification of microscope in measuring the depth

was 100.

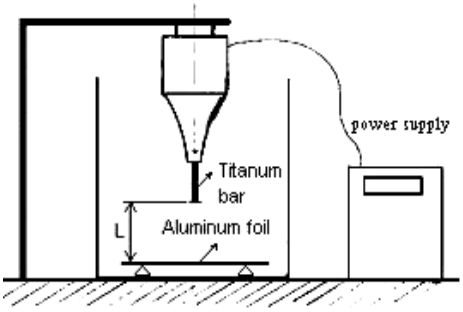

Figure 4. A schematic view of test apparatus

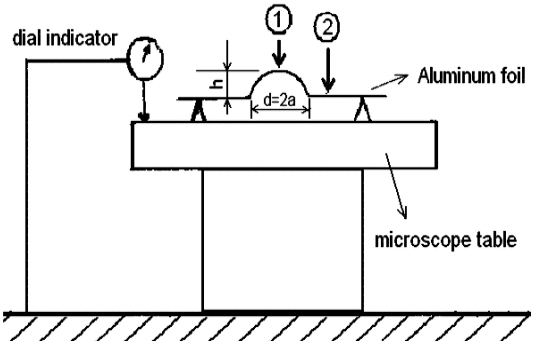

Figure 5. Measuring the depth of a pit

5. Results and Discussion

5.1. Qualitative Observation of Specimens

The largest number of pits and the deepest ones can be observed on specimens located at L=2mm. In the case of L=2mm, the scattered area of pits on the specimen surface decreases as power increases. For powers less than 40 watts, the scattered area is a circle with a diameter of 20mm, and for the power more than this, the scattered area is a circle with a diameter of 8mm. No similar trend was observed in other values of L. On specimen located at L=2mm, at the center of affected zone, pits have been overlapped. Measurement of the dimensions of the pits in this region is difficult and sometimes impossible. Towards the border of the affected zone, the distance between pits increases and the dimension of pits decreases. The number and dimensions of pits, on specimens located at L= ¼ λ=16mm and L= ½ λ=32mm, are smaller than specimens located at L=2mm. Additionally, pits are more scattered on specimens at L= ¼ λ=16mm and L= ½ λ=32mm. At L=2mm, the scattered area of pits decreases as power increases; no similar trend is observed on specimens located at other values of L.

5.2. Observation of Pits under Microscope

Fig. 6 shows the effect of exposure to cavitation on a sample tested at L=2mm and P=40w. As is shown in this figure, the collapse of cavitation bubbles have been produced dome shaped effects on the samples. Two kinds of domes are distinguishable. The first type which is observable on all samples seems to be a part of a sphere whereas the second type can only be seen on samples located at L=2mm and has a conical shape (fig. 7). At L= ½ λ=32mm and L= ¼ λ=16mm, no conical shaped effects have been produced even in high values of P, but at L=2mm, a large number of such effects were produced even in low values of P. So, it seems

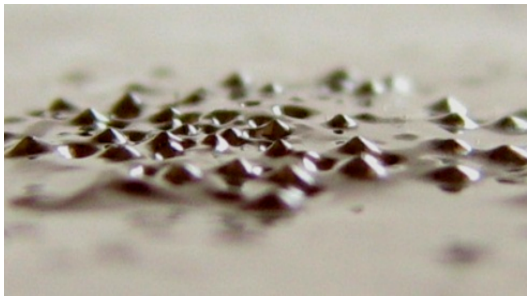

Figure 6. Conical shaped effects on a sample tested at L=2mm, P=40w. This photo has been taken with the angle of 30º from the specimen surface

that the amount of power has no or less effect on the production of conical shaped effects.

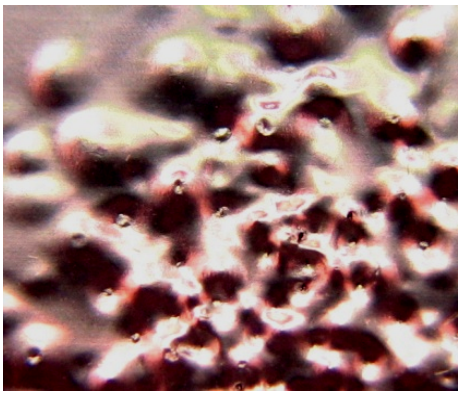

Figure 7. Secondary effects on a specimen tested at L=2mm, P=150w for 10 seconds

Fig. 7 shows a sample which was 2mm apart from horn tip and has been exposed to cavitation for 10 seconds (adjusted power was 150 watts). A kind of secondary pit can be seen on the tip of primary pits. As the time of exposure to cavitation increases, the number of secondary pits increases. Any rupture on the foil will occur in the position of secondary pits.

5.3. Number of Pits

In Fig. 8, the trend of number of pits against adjusted power in different distances is shown. At L= ¼ λ=16mm and L= ½ λ=32mm, an increase in P causes an increase in the number of pits whereas at L=2mm, the number of pits decreases as P increases. A number of pits in the case of L=2mm is much more than L= ¼ λ=16mm and L= ½ λ=32mm.

R^2 value shown in the figure is an indicator from 0 to 1 that reveals how closely the estimated values for the trend line correspond to actual data. A trend line is more reliable when its R-squared value is at or near 1, also known as the coefficient of determination.

5.4. Deformation Energy

Deformation energy, which is required to form the pits on specimens, was calculated through equation 1. Fig. 9 shows maximum energy versus adjusted power. In the case of L=2mm, the greatest energy has been transmitted to specimens by bubbles.

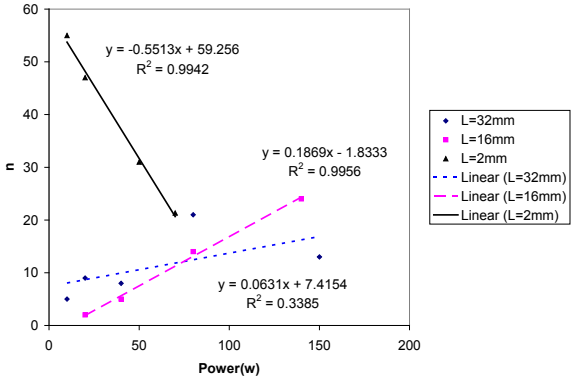

Figure 8. Variation of number of pits with adjusted power in different distances

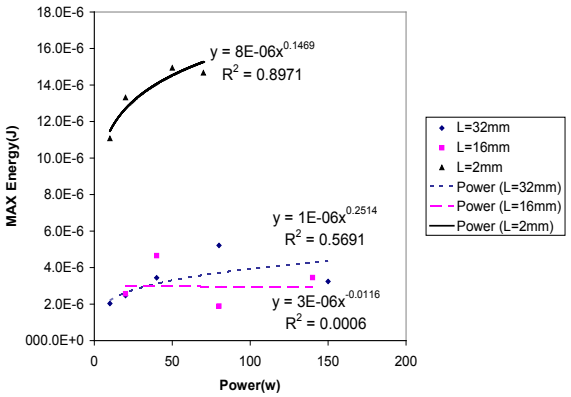

Figure 9. Variation of maximum energy with adjusted power in different distances

Again, curves for L=2mm and L= ½ λ=32mm are similar in both figures. Trend of curves for both maximum and average energy have a similarity with that of microjet. Coefficient of variation of average energy versus adjusted power was plotted. As power increases, coefficient of variation decreases. Interestingly, the slope of straight lines fitted to data is nearly equal in all cases.

5.5. Applied Impulse

The amount of impulse applied to specimens by bubbles was calculated through equation 2. Fig. 28 and Fig. 29 show the maximum and average impulse applied to specimens. Again, the values of impulse at L=2mm is far greater than other cases and L= ¼ λ=16mm has the lowest values. Again, the trend of curves is similar to that of microjet.

REFERENCES

[1] Stoller. M.L., Meng. A.V., Urinary Stone Disease: The Practical Guide to MedicaL and Surgical Management, Humana Press Inc, (2007).

[2] Bailey M.R., Khokhlova V.A., Sapozhnikov O.A., Kargl S.G., Crum L.A., Physical mechanisms of the therapeutic effect of ultrasound (a review). Acoust. Phys., 49, No.4, pp.437-464, (2003)

[3] Christopher E. B., A Review of Cavitation Uses and Problems in Medicine, Cavitation: WIMRC FORUM, (2006)

[4] Jocham, D. Clinical studies documenting renal change after ESWL. In Principles of Extracorporeal Shock Wave Lithotripsy. New York: Churchill Livingstone, pp. 43-47, (1978)

[5] Newman, L.H., Saltzman, B., Identification of Risk Factors in the Development of Clinically Significant Subcapsular Hematomas Following Shock Wave Lithotripsy. In Shock Wave Lithotrispy II: Urinary and Biliary. New York : Plenum Press, pp. 207-210, (1989)

[6] Geert G. T., Management of actue post ESWL complications, Českáurologie (2000)

[7] Delius M., Medical Applications and Bioeffects of Extracorporeal Shock Waves, Shock Waves, (1994)

[8] Evan. A.P., Renal Injury by Extracorporeal Shock Wave Lithotripsy, Journal of Endourology. Vol. 5, pp. 25-35, (1991)

[9] Cullough, D.L. Mc, The bioeffects of Shock Wave Lithotripsy: An Overview. In Shock Wave Lithotripsy II: Urinary and Biliary, Plenum Press, pp. 255-259, (1989)

[10] Desmet, W., Baert, L., Vandeursen, H., Vermeylen, J., Iliac-Vein Thrombosis after Extracorporeal Shock-Wave Lithotripsy. The New England Journal of Medicine

[11] IEC 886 Standard, Investigations on test procedures for ultrasonic cleaners, (1987)

[12] Marciniak Z., Duncan J.L., Hu S.J., Mechanics of sheet metal forming, Butterworth-Heinemann, (2002)

[13] Johnson W., Impact strength of materials, 1st ed. Edward Arnold, pp.176-178, (1972)

[14] Baghizadeh E., Abdullah A., Investigation of ultrasonic cavitation impact on solid surfaces, M.Sc. Thesis, AmirKabir University of Technology, (2007)